

Electromagnetically induced walking

Wenxi Lai*

School of Applied Science, Beijing Information Science and Technology University, Beijing 100192, China

In atomic devices, momentum uncertainty of atom wave packet gives rise to Doppler broadening which influences the control of atoms with light. Here, we use a Rydberg-atom to show that strong coupling between atom-light interactions located in the synthetic dimensional topological edge state can avoid the affect from Doppler broadening, inducing coherent periodic motion of atom center of mass. Oscillating potential for the atom walking directly comes from the back action process. These results may be important for the development of atomtronic circuits.

PACS numbers: 37.10.Vz, 32.90.+a, 3.75.-b, 42.50.Ct

Atomtronics is an emerging technique in which atoms are believed to be controllable and useful analogous to electrons in electronics. This property of atomtronics make it have potential applications in many areas and attract great attentions in recent decade, such as atomtronic transistors [1–4], circuits [5–7], SQUID [8–10], batteries [11–13], interferometry [14–16], hole states [17] and qubit [18].

In atomtronic circuits, control and transport of atoms always relate to the real space freedoms. In infinite volume free-space, an atom should move as a plane wave with definite momentum. However, in a practical materials or devices, an atom should be described by a wave packet as its position is localized in a finite volume [16, 19]. It naturally leads to momentum uncertainty according to the Heisenberg uncertainty principle $\Delta x \Delta p \sim h$. In atom-light coupling, the momentum uncertainty of the wave packet causes Doppler broadening to atom transition levels, which seriously influences the efficiency of control and coherence of atom wave packet [20].

In this paper, we show that strong coupling of atom-light interaction can avoid the influence from Doppler broadening and back action offers oscillating potential to the atom, which induce coherent walking of the atom in continuum. We may call it electromagnetically induced walking (EIW). The EIW occurs around the energy of synthetic dimensional topological edge states. The topological edge states in synthetic dimensions of ultracold ^{84}Sr atom has been experimentally observed quite recently [21].

There are some similarities between EIW and EIT (electromagnetically induced transparency). In the EIT [22, 23], a strong coupling laser shift the broadened level in medium by ac-Stark splitting, which make a weak probe laser with the common transition level transit through the medium. Without the coupling field, the weak probe laser would be absorbed by the medium. In the EIW, when a laser field strong enough to shift a Doppler broadened level, the atom would coherently

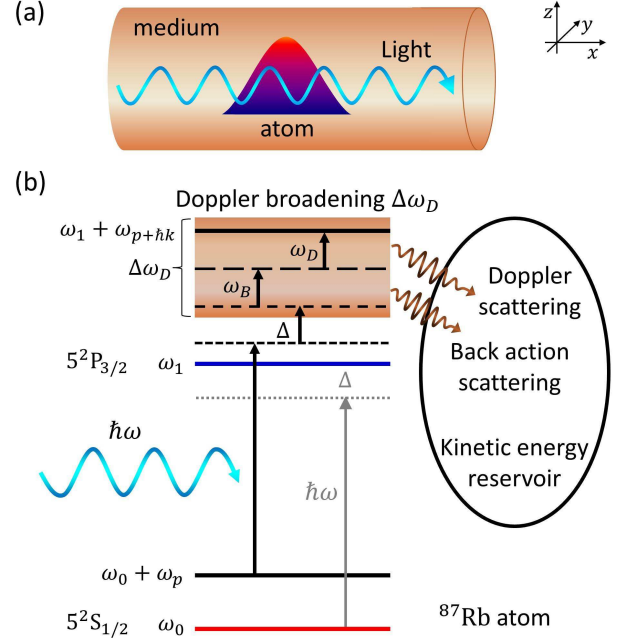


FIG. 1: (Color on line) (a) Schematic illustration of light acting on an atom wave packet in a homogeneous medium or waveguide. (b) Energy structure of atom-light coupling associated with kinetic energy reservoir.

walk in the real space. Otherwise, the atom is hard to walk in the kinetic energy reservoir.

In our model, environmental influences are characterized by wave packet of an atom as conceptually shown in Fig. 1 (a). In dark environment that before the atom interacts with light, we suppose the wave packet is a Gaussian function $|\Psi(0)\rangle = \int dp \sum_n \Psi_n(p, 0) |n, p\rangle$, where the probability distribution function is $\Psi_n(p, 0) = \frac{C_n}{\pi^{1/4} \sqrt{\Pi}} e^{-(p-p_c)^2/2\Pi^2}$. C_n denotes probability amplitude of the internal electronic state $|n\rangle$. p_c represents the center momentum. The characteristic momentum Π is determined by the dark environment. Under the action of light, motion of an atom would be described by the wave function $|\Psi(t)\rangle = \int dp \sum_n \Psi_n(p, t) |n, p\rangle$. Evolution of the wave function satisfies the Schrödinger equation $i\hbar \frac{\partial}{\partial t} |\Psi(t)\rangle = \mathbf{H} |\Psi(t)\rangle$ with the Hamiltonian

*Electronic address: wxlai@pku.edu.cn

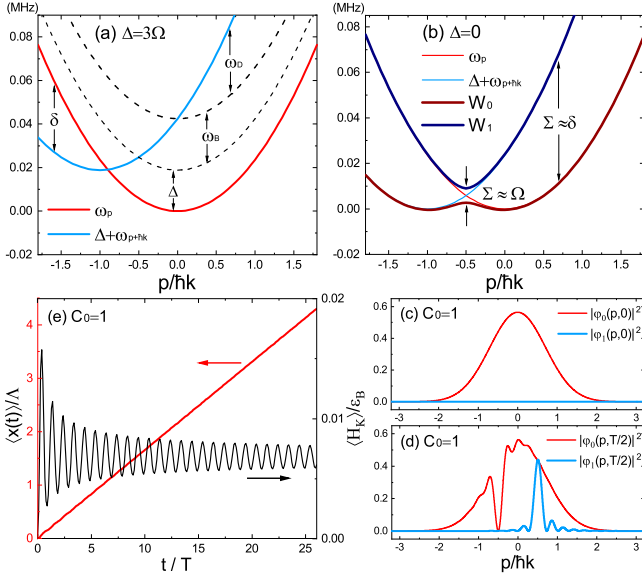


FIG. 2: (Color on line) (a) Energy structure in the interaction picture. (b) Relation between eigenfrequencies and the original transition levels. (c)-(e) Displacement, kinetic energy of the atom as a function of time and corresponding change in the probability distribution functions, where $\Delta = 0$. The common parameters are $\Omega = 2\pi \times 1$ KHz, $\Pi = \hbar k$ and $p_c = 0$.

$\mathbf{H} = \mathbf{H}_e + \mathbf{H}_K + \mathbf{H}_I$. The first term \mathbf{H}_e represents energy of the electronic motion in atom with eigenvalue $\hbar\omega_n$ and eigenstate $|n\rangle$. Here, electron in the atom is an open system whose reservoir is the kinetic motion of the atom wave packet described by the Hamiltonian,

$$\mathbf{H}_K = \int dp \frac{p^2}{2M} |p\rangle\langle p|, \quad (1)$$

where M is atom mass. As illustrated in Fig. 1 (b), we consider the transition $5^2S_{1/2} \rightarrow 5^2P_{3/2}$ of Rubidium (^{87}Rb) atom with resonant wave length 780 nm [24, 25] and dipole moment $|\mu| = 3.584 \times 10^{-29}$ C·m [26]. This internal electronic transition would couple to the kinetic energy reservoir of the wave packer under the electromagnetic field $\vec{\mathbf{E}}(\mathbf{x}, t) = \vec{\mathbf{e}}_z E_0 \cos(\omega t - kx)$, which can be described by the interacting Hamiltonian,

$$\mathbf{H}_I = -\frac{\hbar}{2} \int dp (\Omega e^{-i\omega t} |1, p + \hbar k\rangle\langle 0, p| + H.c.), \quad (2)$$

where the Rabi frequency is $\Omega = \mu E_0 / \hbar$ with dipole moment of the atom $\mu = \langle 0 | e \mathbf{z} | 1 \rangle = |\mu| e^{i\phi}$ [27]. The initial phase would be taken to be $\phi = 0$ for convenience of discussion. In derivation of Eq.(2), the relation of momentum displacement operator $e^{\pm ikx} |p\rangle = |p \pm \hbar k\rangle$ has been used [28].

To solve the wave function $|\Psi(t)\rangle$, the original Schrödinger equation can be written into interaction picture $i\hbar \frac{\partial}{\partial t} |\varphi(t)\rangle = \mathbf{V} |\varphi(t)\rangle$ with the wave function $|\varphi(t)\rangle = e^{i\mathbf{H}_0 t / \hbar} |\Psi(t)\rangle$ and time independent Hamiltonian $\mathbf{V} = e^{i\mathbf{H}_0 t / \hbar} \mathbf{H}_I e^{-i\mathbf{H}_0 t / \hbar}$, where the corresponding

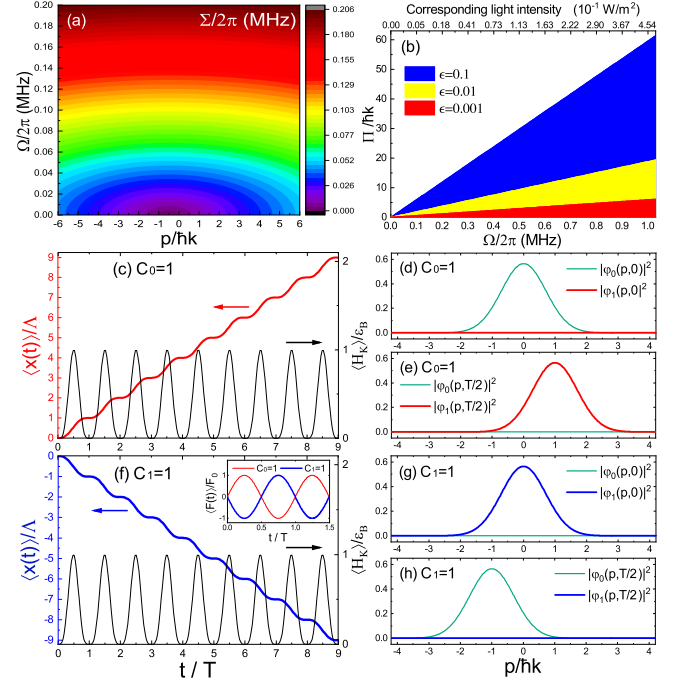


FIG. 3: (Color on line) (a) The energy gap Σ as a function of the Rabi frequency Ω and atom momentum p . (b) Illustration of strong coupling and weak coupling regimes. Displacement, kinetic energy of the atom as a function of time and corresponding change in the probability distribution functions with the initial state $C_0 = 1$ in (c)-(e) and with the initial state $C_1 = 1$ in (f)-(h). The inset figure in (f) shows optical forces acting on the atom for different initial states. The common parameters are $\Omega = 2\pi \times 1$ MHz, $\Pi = \hbar k$, $p_c = 0$ and $\Delta = 0$.

unitary operator is $\mathbf{H}_0 / \hbar = \omega_0 |0\rangle\langle 0| + (\omega_0 + \omega) |1\rangle\langle 1|$. The wave function $|\varphi(t)\rangle$ can be expanded with probability distribution functions as $|\varphi(t)\rangle = \int dp \sum_n \varphi_n(p, t) |n, p\rangle$. For a definite momentum p , the Schrödinger equation in interaction picture reduced into a differential equation of 2×2 matrix in the sub space of $\{|0, p\rangle, |1, p + \hbar k\rangle\}$ as

$$i \begin{bmatrix} \dot{\varphi}_{0,p}(t) \\ \dot{\varphi}_{1,p+\hbar k}(t) \end{bmatrix} = \begin{bmatrix} \omega_p & -\frac{\Omega}{2} \\ -\frac{\Omega}{2} & \Delta + \omega_{p+\hbar k} \end{bmatrix} \begin{bmatrix} \varphi_{0,p}(t) \\ \varphi_{1,p+\hbar k}(t) \end{bmatrix}, \quad (3)$$

where $\omega_p = \frac{p^2}{2M\hbar}$, $\omega_{p+\hbar k} = \frac{(p+\hbar k)^2}{2M\hbar}$ and the detuning $\Delta = \omega_1 - \omega_0 - \omega$. Eq.(3) can be easily diagonalized and the eigenfrequencies are $W_{0,1} = \frac{1}{2}(\omega_p + \omega_{p+\hbar k} + \Delta \mp \sqrt{(\omega_p - \omega_{p+\hbar k} - \Delta)^2 + \Omega^2})$. From Eq.(3) one could solve the wave function $|\varphi(p, t)\rangle = \varphi_{0,p}(t) |0, p\rangle + \varphi_{1,p+\hbar k}(t) |1, p + \hbar k\rangle$ for a given initial state $|\Psi(0)\rangle$.

In the energy structure of this system, transition frequency $\delta = \Delta + \omega_{p+\hbar k} - \omega_p$ is composed of the detuning Δ , the back action shift $\omega_B = \frac{\hbar k^2}{2M}$ and the Doppler shift $\omega_D = \frac{Pk}{M}$ in the form $\delta = \Delta + \omega_B + \omega_D$ as illustrated in Fig. 2 (a). Since the Doppler shift is proportional to the momentum of wave packet which has continuous probability distribution in momentum space, the optical transition levels would have the Doppler broadening $\Delta\omega_D = \frac{2\Pi\hbar k}{M}$ related to the characteristic momentum Π

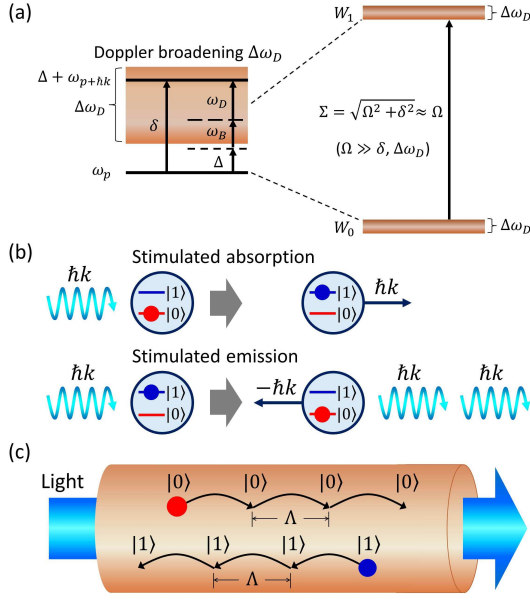


FIG. 4: (a) The principle of strong coupling in the system. (b) Illustration of spin-orbit coupling during the atom-photon interactions. (c) Walking of atom in the opposite directions due its different initial internal states $|0\rangle$ and $|1\rangle$.

of the wave packet (see Fig. 1 (b)). In the transition frequency δ , the back action shift can be removed by taking the detuning $\Delta = -\omega_B$. However, the Doppler broadening $\Delta\omega_D$ can't be removed simply by tanking a detuning Δ due to its momentum uncertainty.

From the point of view of eigenfrequencies as shown in Fig. 2 (b), the eigenfrequency difference $W_2 - W_1 = \sqrt{\delta^2 + \Omega^2}$ gives two regimes, the weak coupling regime $\delta \gg \Omega$ and the strong coupling regime $\delta \ll \Omega$. By denoting $\Sigma = W_2 - W_1$, this two regimes can be analyzed from the elliptic equation,

$$\frac{\left(\frac{p}{\hbar k} + \frac{\Delta}{2\omega_B} + \frac{1}{2}\right)^2}{\left(\frac{\Sigma}{2\omega_B}\right)^2} + \frac{\Omega^2}{\Sigma^2} = 1, \quad (4)$$

which has been plotted in Fig. 3 (a). The figure reveals the weak and strong coupling regimes are relative. For larger momentum range $-\Pi < p + \frac{\Delta}{2\omega_B} + \frac{1}{2} < \Pi$, a larger Rabi frequency Ω is required to satisfy the strong coupling regime. As indicated in Fig. 2 (b), in the strong coupling regime $\Sigma \approx \Omega$ which is around the topological edge-state energy [29]. The critical momentum Π is determined by the wave packet $|\Psi(t)\rangle$. To find the quantitative relation between the critical momentum Π and the Rabi frequency Ω , an infinitely small parameter ϵ could be defined, for which $\Sigma \leq \Omega(1+\epsilon)$. It guarantee Σ is close to Ω infinitely. Then from Eq.(4) we have the criteria of the Rabi frequency Ω for any characteristic momentum Π of a wave packet,

$$\Omega \geq \frac{\sqrt{2}\omega_B}{\sqrt{\epsilon}} \left(\frac{\Pi}{\hbar k} + \frac{\Delta}{2\omega_B} + \frac{1}{2} \right). \quad (5)$$

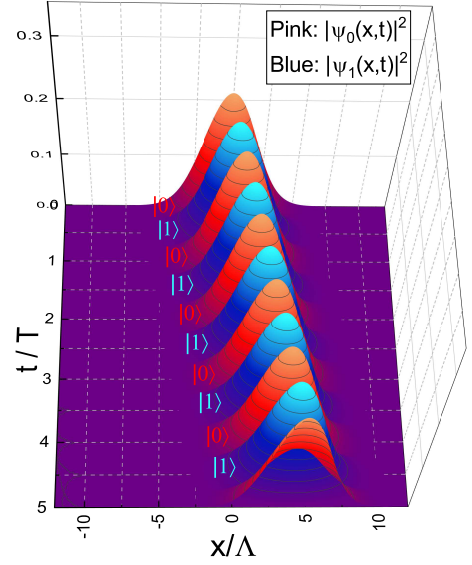


FIG. 5: (Color on line) Periodic displacement of the atom wave packet along with time in the x coordinate of real space.

In Fig. 3 (b), the area given by inequality Eq.(5) has been plotted for the detuning $\Delta = -\omega_B$.

In Fig. 3 (c-h), the values of Rabi frequency $\Omega = 2\pi \times 1$ MHz and characteristic momentum $\Pi = \hbar k$ are taken, which satisfy the inequality Eq.(5) at the parameter $\epsilon = 0.001$ as revealed in Fig. 3(b). As a result, almost fully periodic motion of the atom wave packet has appeared as shown in Fig. 3 (c) and (f). Expectation value of the wave packet momentum has been calculated through the formula $\langle p(t) \rangle = \langle \varphi(t) | p | \varphi(t) \rangle$. In the strong coupling regime $\delta \ll \Omega$, it has the simple form,

$$\langle p(t) \rangle = p_c + (C_0^2 - C_1^2) \hbar k \sin^2\left(\frac{\Omega t}{2}\right). \quad (6)$$

From the function of momentum $\langle p(t) \rangle$ one can obtain displacement of the atom,

$$\langle x(t) \rangle = \langle x(0) \rangle + \frac{2p_c \Lambda t}{\hbar k T} + (C_0^2 - C_1^2) \Lambda \left(\frac{t}{T} - \frac{\sin\left(\frac{2\pi t}{T}\right)}{2\pi} \right), \quad (7)$$

with the step length $\Lambda = \frac{\pi \hbar k}{M \Omega}$ and the periodicity $T = \frac{2\pi}{\Omega}$. The optical force acting on the atom,

$$\langle F(t) \rangle = (C_0^2 - C_1^2) F_0 \sin(\Omega t), \quad (8)$$

with the force amplitude $F_0 = \frac{1}{2} \hbar k \Omega$.

From Eq.(7), static atoms in the ground state $|0\rangle$ and excited state $|1\rangle$ move in opposite direction under the action of a propagating light just like the positively and negatively charged particles move in opposite directions under the action of an electric field. The initial state dependent behavior coincides with the spin-orbit coupling in the synthetic dimensions of optical lattice [30] and continuum [31]. The oscillating forces acting on the atom with different states have phase difference of π as shown in the inset of Fig. 3 (f). Kinetic energy changes of

the wave packet plotted in Fig. 3 (c) and (f) reveal that energy of the atom walking comes from the back action effect. As illustrated in Fig. 3 (d), (e), (g), (h) with the evolution of the wave function, the energy exchange is occurred during the stimulated absorption and stimulated emission of photon within the half periodicity $\frac{T}{2} = \frac{\pi}{\Omega}$, respectively. This process in the strong coupling regime is conceptually illustrated in Fig. 4. Step length Λ of the EIW is related to momentum $\hbar k$ of a photon, atom mass M and Rabi frequency. Clearly, it can be tuned arbitrarily with the Rabi frequency for a given atom.

Evolution of the wave function in real space could be describe with the wave function in position space $|\psi(x, t)\rangle = \psi_0(x, t)|0\rangle + \psi_1(x, t)|1\rangle$, where the amplitudes are obtained through the fourier transformation $\psi_0(x, t) = \int dp \varphi_0(p, t)\langle x|p\rangle$ and $\psi_1(x, t) = \int dp \varphi_1(p, t)\langle x|p\rangle$. Displacement of the wave function in x coordinate is shown in Fig. 5. The wave packet with a position uncertainty is moving periodically along with the transition of the internal states of the atom.

The walking process is similar to a longitudinal wave whose wave length is Λ and frequency is $f = T^{-1}$. Through the concept of longitudinal wave, speed of the atom walking is $v = f\Lambda$ which gives a Rabi frequency independent result $v = \frac{\hbar k}{2M}$. For the transition $5^2S_{1/2} \rightarrow 5^2P_{3/2}$ of the ^{87}Rb atom the step length can be estimated to be $\Lambda = 292.34$ nm, 29.23 nm and 2.92 nm for the Rabi frequency $\Omega = 2\pi \times 0.01$ MHz, $2\pi \times 0.1$ MHz and $2\pi \times 1$ MHz, respectively. In this case, the speed of the wave packet should be $v = 2.92 \times 10^6$ nm/s. Considering

the many-atom process in atomtronic circuits, our model is suitable to describe low density atomic gas where atom-atom interaction becomes negligible small [32, 33].

There is difference between the EIW and quantum walk of neutral atoms. The quantum walk of neutral atoms describes random walk of atoms commonly in optical lattice [34, 35]. However, EIW is a coherent walk of atoms in continuum with a definite phase and controllable step length.

In summary, we proposed the electromagnetically induced walking of single atoms, in which an atom coherently walks overcoming environmental noise through Doppler effects. The EIW mainly has following properties. First, step length of the walking and time periodicity can be tuned arbitrarily with the Rabi frequency. Second, the direction of atom walking is determined by the initial state of internal electronic state. Third, the strong coupling of atom-light interaction for the coherent atom walk is located in the topological edge state. Forth, the highest kinetic energy of the atom center of mass during the walking process is equal to the back action energy.

Acknowledgments

This work was supported by the Scientific Research Project of Beijing Municipal Education Commission (BMEC) under Grant No.KM202011232017.

-
- [1] R. A. Pepino, J. Cooper, D. Z. Anderson, M. J. Holland, Phys. Rev. Lett. **103** (2009) 140405.
 - [2] M. Fuechsle, J. A. Miwa, S. Mahapatra, et al., Nature Nanotech. **7** (2012) 242.
 - [3] Andrew J. Daley, Physics **8** (2015) 72.
 - [4] Dana Z. Anderson, Phys. Rev. A **104** (2021) 033311.
 - [5] Jeffrey G. Lee, Brian J. McIlvain, C. J. Lobb, W. T. Hill, Sci. Rep. **3** (2013) 1034.
 - [6] Weng W. Chow, Cameron J. E. Straatsma, Dana Z. Anderson, Phys. Rev. A **92** (2015) 013621.
 - [7] Enrico Compagno, Guillaume Quesnel, Anna Minguzzi, Luigi Amico, Denis Feinberg, Phys. Rev. Research **2** (2020) 043118.
 - [8] Davit Aghamalyan, Marco Cominotti, Matteo Rizzi, et al., New J. Phys. **17** (2015) 045023.
 - [9] C. Ryu, E. C. Samson, M. G. Boshier, Nat. Commun. **11** (2020) 3338.
 - [10] D. M. Jezek, H. M. Cataldo, Phys. Rev. A **104** (2021) 053319.
 - [11] Alex A. Zozulya, Dana Z. Anderson, Phys. Rev. A **88** (2013) 043641.
 - [12] Seth C. Caliga, Cameron J. E. Straatsma, Dana Z. Anderson, New J. Phys. **19** (2017) 013036.
 - [13] Wenxi Lai, Yu-Quan Ma, Lin Zhuang, W. M. Liu, Phys. Rev. Lett. **122** (2019) 223202.
 - [14] L. P. Parazzoli, A. M. Hankin and G. W. Biedermann, Phys. Rev. Lett. **109** (2012) 230401.
 - [15] J. E. Palmer and S. D. Hogan, Phys. Rev. Lett. **122** (2019) 250404.
 - [16] M. D. Lachmann, H. Ahlers, D. Becker, et al., Nat. Commun. **12** (2021) 1317.
 - [17] A. Benseny, S. Fernández-Vidal, J. Bagudà, R. Corbalán, A. Picón, L. Roso, G. Birkel, and J. Mompart, Phys. Rev. A **82** (2010) 013604.
 - [18] S. Safaei, B. Grémaud, R. Dumke, L.-C. Kwek, L. Amico, C. Miniatura, Phys. Rev. A **97** (2018) 042306.
 - [19] G. L. Gattobigio, A. Couvert, G. Reinaudi, B. Georgeot, and D. Guéry-Odelin, Phys. Rev. Lett. **109** (2012) 030403.
 - [20] Hermann Uys, John D. Perreault, and Alexander D. Cronin, Phys. Rev. Lett. **95** (2005) 150403.
 - [21] S. K. Kanungo, J. D. Whalen, Y. Lu, et al., Nat. Commun. **13** (2022) 972.
 - [22] K.-J. Boiler, A. Imamoğlu, and S. E. Harris, Phys. Rev. Lett. **66** (1991) 2593.
 - [23] Wen-Xi Lai, Hong-Cai Li, Rong-Can Yang, Opt. Commun. **281** (2008) 4048.
 - [24] Jun Ye, Steve Swartz, Peter Jungner, and John L. Hall, Opt. Lett. **21** (1996) 1280.
 - [25] J. E. Sansonetti and W. C. Martin, J. Phys. Chem. Ref. Data **34** (2005) 1559.
 - [26] Daniel A. Steck, Rubidium 87 D Line Data, 2003.
 - [27] M. O. Scully and M. S. Zubairy, Quantum Optics, Cambridge University Press, Cambridge, 1997.

- [28] P. Meystre and M. Sargent III, *Elements of Quantum Optics*, Springer-Verlag, Berlin Heidelberg, 2007.
- [29] Ching-Kai Chiu, Jeffrey C. Y. Teo, Andreas P. Schnyder, and Shinsei Ryu, *Rev. Mod. Phys.* **88** (2016) 035005.
- [30] Michael L. Wall, Andrew P. Koller, Shuming Li, Xibo Zhang, Nigel R. Cooper, Jun Ye, and Ana Maria Rey, *Phys. Rev. Lett.* **116** (2016) 035301.
- [31] L. Huang, Z. Meng, P. Wang, et al., *Nature Phys.* **12** (2016) 540.
- [32] G. L. Gattobigio, A. Couvert, M. Jeppesen, R. Mathevet, and D. Guéry-Odelin, *Phys. Rev. A* **80** (2009) 041605.
- [33] A. Couvert, M. Jeppesen¹, T. Kawalec, G. Reinaudi, R. Mathevet and D. Guéry-Odelin, *Europhys. Lett.* **83** (2008) 50001.
- [34] W. Dür, R. Raussendorf, V. M. Kendon, and H.-J. Briegel, *Phys. Rev. A* **66** (2002) 052319.
- [35] Michal Karski, Leonid Förster, Jai-Min Choi, et al., *Science* **325** (2009) 174.